Effect of Surface Finish on Fatigue of Stainless Steels

S. Al-Shahrani, and T.J. Marrow
The University of Manchester, School of Materials, Manchester, UK;

ABSTRACT

The effect of surface finish on fatigue limit of Type 304 austenitic stainless steels has been investigated. Fatigue specimens with different surface conditions were obtained by changing the final cutting condition of lathe-turning. The surfaces and near surface microstructures were characterised by electron backscatter diffraction (EBSD), surface profilometry, hardness testing and X-ray diffraction for residual stress measurement. The fatigue limits were determined using a rotating-bending machine by means of the staircase method. Machined samples were compared with samples annealed to remove residual stresses, and also samples that were annealed and electro-polished. Arrested crack nuclei in run-out ($>10^7$ cycles) fatigue tests were observed. The residual stress measured at the surface was found to be the dominant parameter, which changes the fatigue limit relative to that of electropolished and annealed microstructures. The effect of surface roughness is negligible.

1. INTRODUCTION

The fatigue resistance of austenitic stainless steels is critical to the performance of pipework and cladding in heat exchangers and cooling systems. Surface machining is common in such components, and it is important to be able to assess the likely effects of surface treatments. This paper reports part of a research program that aims to predict the effects of the surface finish on fatigue in these materials. In previous work [1]-[3] two different examples of type 304 stainless steel, with different grain size, were employed in a study of the effect of surface finish on high cycle, stress controlled fatigue. The results indicated insensitivity to surface finish and sensitivity to the surface residual stress. However, a general model could not be developed as different machining conditions were not examined in a single microstructure. In this report, a third type of 304L austenitic stainless steel has been studied in order to obtain data for one microstructure with different surface finishes. The results are compared with the earlier studies.

The fatigue specimens were designed using a response surface, which gave an empirical prediction of the effects of machining parameters on roughness and surface residual stress [4]. This had been developed in machining studies of a different microstructure of type 304 stainless steel, and one objective of this work was to test its generality to other type 304 steel microstructures. Electron backscatter diffraction (EBSD), surface profilometry, hardness testing and X-ray diffraction residual stress measurement were employed to characterise the surface and microstructures. The fatigue limits were determined using a rotating-bending machine by means of the staircase method.

2. MATERIALS AND EXPERIMENTAL PROCEDURE

The material used was an austenitic stainless steel (AISI 304L) supplied in the form of a round bar (dia. 10 mm). The chemical composition is given in Table 1. The grain size was measured from optical micrographs using the linear intercept method. Mechanical properties were obtained using tensile specimens with a gauge diameter of 5 mm, a gauge length of 30 mm and a displacement rate of 2 mm/min.

Table 1: Chemical composition of the stainless steel employed (wt %)

Source of Data	C	P	S	Si	Mn	Cr	Ni	Mo	N	Fe
AISI 304L	0.028	0.030	0.030	0.32	1.3	18.365	8.53	0.39	0.077	Bal.

The geometry of fatigue specimens is given in Figure 1. These were prepared by a numerically controlled lathe. Two different conditions of surface roughness and surface residual stress were produced by changing the final cutting conditions (spindle speed, feed rate and cutting depth). The spindle speed (1500r/min) and cut depth (0.4 mm) were the same for both conditions, with a feed rate of 0.25 mm/revolution for the rough machined condition (R) and 0.1 mm/rev for the fine machined condition (F). The tip radius of insert tool was 0.4 mm. These conditions were selected from the response surface [4] to obtain residual stresses that were either close to zero (fine machined) or tensile (rough machined).

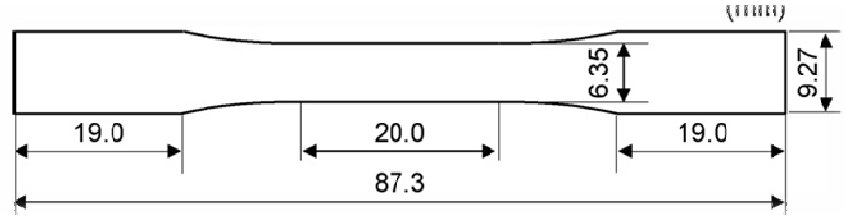

Figure 1: Specimen configuration (circular cross-section).

Surface roughness profiles of machined specimens were characterised using a Taylor-Hobson Talysurf 50 surface Profilometer. The microhardness was measured using an Instron indentation instrument (Wilson model Tukon 2100), with an applied load and load time of 500 g and 10 s, respectively. The residual stress was measured by the $\sin^2\psi$ method was using a Proto i-XRD x-ray difractometer. The $\{311\}_{hkl}$ planes were selected at a Bragg reflection of 156^o (2θ) using a Mn-Kα radiation tube with a wavelength λ=0.21nm. The acceleration voltage was 20KV with a current of 4mA. A 1 mm collimator was used. Depth profiles of residual stress were obtained using successive electropolishing at intervals of approximately 30 μm. The Young's modulus and Poisson's ratio employed were 193 GPa and 0.29, respectively. No correction was carried out to account for the material removal of surface layers. However, the effect of neglecting this was calculated to be less than 7 % [5]. Sets of fatigue specimens were annealed at 900°C for 10 minutes under an argon gas flow. Other

specimen sets were similarly annealed and then electrochemically polished to remove approximately 150 µm from the diameter. Residual stress measurements were obtained from at least two independent specimens for each condition.

The fatigue limits were determined on a R.R Moore rotating-bending machine using the staircase method with sets of 20 specimens, employing a step-width of 2 MPa. The fatigue endurance limit was set at 10^7 cycles. Scanning electron microscopy (SEM) was used for fractography and examination of specimens after fatigue testing, while SEM and Electron Backscattered Diffraction (EBSD) were used to study the microstructures close to the surface in sectioned metallographic specimens. These were first electroplated with approximately 100 µm Ni to improve edge retention. An HKL-EBSD system with a low light CCD camera (Nordlys II), interfaced to a Philips XL-30 FEG-SEM was used for this assessment. Data were acquired using Channel 5 Flamenco HKL software in the beam scanning mode, with an accelerating voltage of 20 kV and a 100 µm aperture. The acquisition time was set to 60 ms per point, with a step size of 0.5 µm.

3. RESULTS

The grain size of this microstructure was 56 µm (standard deviation 7 µm). The measured tensile properties are summarised in Table 2, and are similar to the expected values. The measured surface parameters are given in Table 3. The rough machined surface has significant tensile residual stress (~260 MPa) in comparison to the fine machined surface (~50 MPa). The expected surface stresses, predicted using the response surface [4] for these machining conditions were 280 MPa and 0 MPa, respectively. Similar hardness levels were found for both machining conditions, and these were reduced significantly by annealing. The lowest hardness was measured after electro-polishing the annealed microstructure.

The variation of axial residual stress with depth is shown in Figure 2. Both machining conditions produce a compressive residual stress peak of approximately 350 MPa, which is closer to the surface in the fine machined condition. No significant residual stresses were observed beyond approximately 400 µm from the surface. Annealing effectively eliminates the residual stresses induced by machining. The width of the {311} diffraction peaks (measured as the Full Width at Half Maximum intensity, i.e. FWHM) is shown in Figure 3. Higher values are obtained within 150 to 200 µm of the surface in the machined samples, and are removed by annealing.

Table 2: Mechanical properties of type 304L (as-received). Two samples tested.

Material	**0.2% Proof Stress [MPa]**	**Ultimate Tensile Strength [MPa]**
Measured in this work	541 & 547	707& 711

Table 3:Parameters of machined surfaces (± one standard deviation).

Surface residual stress (MPa)	Fine Machined	50±44
	Rough Machined	260±56
	Electropolished	3±40
	Fine Machined (Annealed)	-50±24
	Rough Machined (Annealed)	-14±25
Roughness, Ry (µm) *(Maximum peak to valley height)*	Fine Machined	7±1
	Rough Machined	23±1
Roughness, S (µm) *(Average peak spacing)*	Fine Machined	26±2
	Rough Machined	83±6
Microhardness, Hv	Fine Machined	321±2
	Rough Machined	347±4
	Electropolished*	152±2
	Fine Machined (Annealed)	176±3
	Rough Machined (Annealed)	189±5

*Fine machined, annealed and then electropolished to remove 75µm from surface.

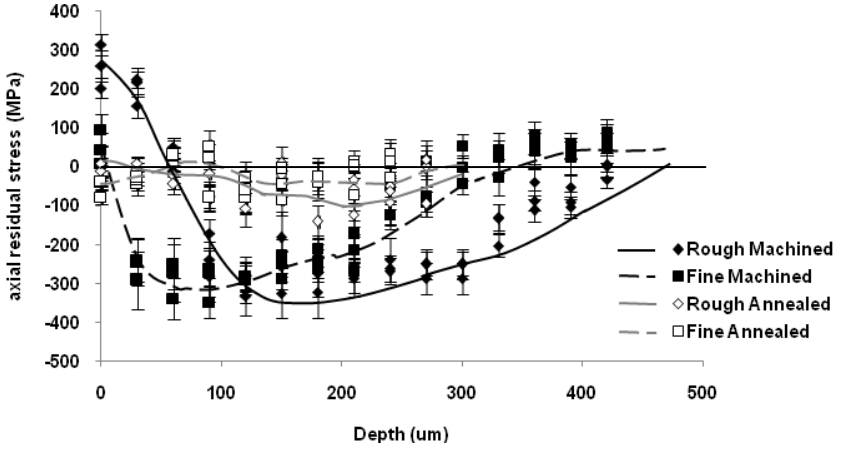

Figure 2: Variation of axial residual stress with depth for machined and annealed surfaces. Approximate trend lines added for visualisation.

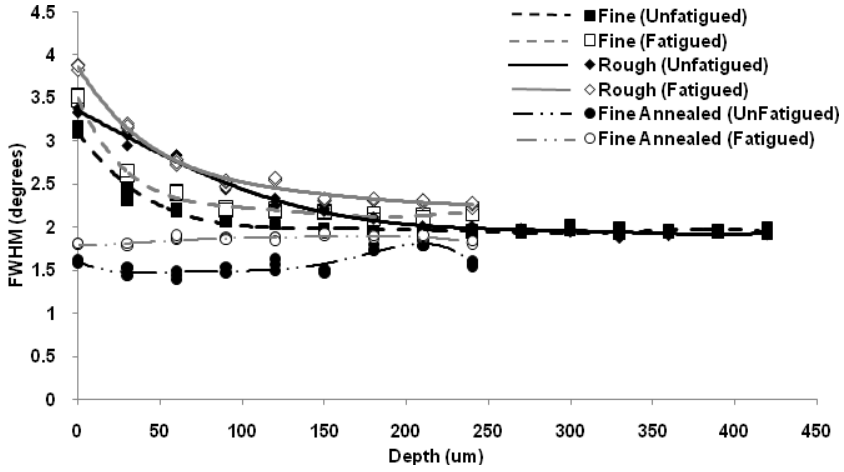

Figure 3: Variation of {311} diffraction peak width (FWHM) with depth.

The lowest fatigue limit was measured in the rough machined condition (Table 4). The fatigue limits for the other surfaces did not differ significantly from each other. Surface and metallographic observations of longitudinal sections from run out (10^7 cycles) specimens (Figure 4) show crack-like features in all cases. These tended to be quite linear in the electro-polished and fine machined conditions, but features with a more irregular profile were observed on the rough machined surfaces.

Table 4: Fatigue limits obtained by staircase method (± one standard deviation).

Condition	**Fatigue Limit (MPa)**
Fine Machined	327±8
Fine Machined & Annealed	343±18
Fine Machined & Annealed & Electropolished	337±2
Rough Machined	291±3
Rough Machined & Annealed	337±1

.

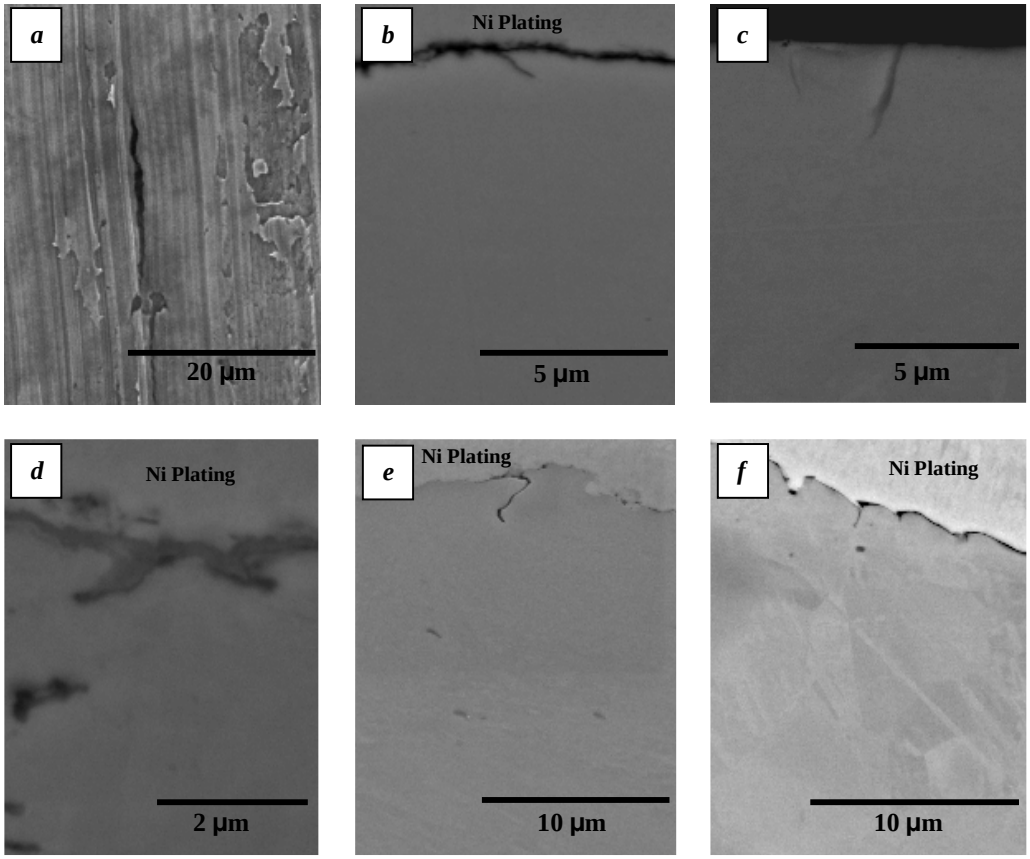

Figure 4: Crack-like features in fatigued (run-out) specimens: a) Fine machined (surface observation), b) Fine machined, c) Electropolished, d) Annealed (Fine machined), e) Rough machined, f) Annealed (Rough machined).

The Kikuchi "band contrast" maps obtained by EBSD (Figure 5) are sensitive to plastic strain and can be used to reveal slip bands [6] [7]. The intensity of band contrast was highest close the machined surfaces, and was not noticeably affected by fatigue cycling. Slip bands were evident, prior to fatigue testing, in the bulk microstructure both before and after annealing. The density of these slip bands was reduced in the annealed samples. Fatigue to run-out appeared to cause a slight increase in the density of slip bands (Figure 5), although this could not be quantified reliably.

4. DISCUSSION

The measured surface residual stresses of 50 ± 45 MPa and 260 ± 50 MPa are in fair agreement with the stresses of 0 MPa and 280 MPa predicted by the response surface model. This empirical model was developed using different grades of type 304 austenitic stainless steel, and machining tools of the same 0.4 mm radius from a different manufacturer [4]. The measurements demonstrate that the response surface is a quite robust tool for estimating the effects of machining on the surface residual stress. The use of a fresh tool tip for the final cut on each specimen gave a small standard deviation in the measured fatigue limit, thereby allowing differences between the surfaces to be determined reliably.

The measured surface and microstructure parameters were used to calculate the fatigue crack propagation threshold stress for each condition, using the implementation of the Navarro-Rios (N-R) short fatigue crack model. The methodology is described in detail in reference [1]. An important aspect of the model is the assumption that the austenite grain boundaries act as barriers to crack propagation. The grain size is the average barrier spacing. The N-R short crack model is most sensitive to factors with a similar length scale to the barrier spacing. This causes the compressive residual stress peak from machining to have a significant effect on crack propagation, as well as the stress concentration from the surface roughness [1]. The peak threshold value for each condition is the minimum stress amplitude for unstable crack propagation, which is the fatigue limit (Figure 6). The model predicts significant differences between the conditions, but does not agree with the experimental observations (Figure 6). This is consistent with previous observations in austenitic stainless steels [2] [3].

Although the irregular features observed in the rough machined samples (e.g. Figure 4d) are likely to be defects introduced by machining, the crack-like features in the electropolished samples are clearly due to fatigue. Features such as those observed in the fine machined samples after fatigue also were not observed in samples that had not been fatigued, and are concluded to be fatigue cracks. The irregular defects in the rough machined samples would be significant stress raisers, and are assumed to act as crack nuclei. All samples therefore show that stable crack nuclei with a size of a few µm existed after run-out at the fatigue limit.

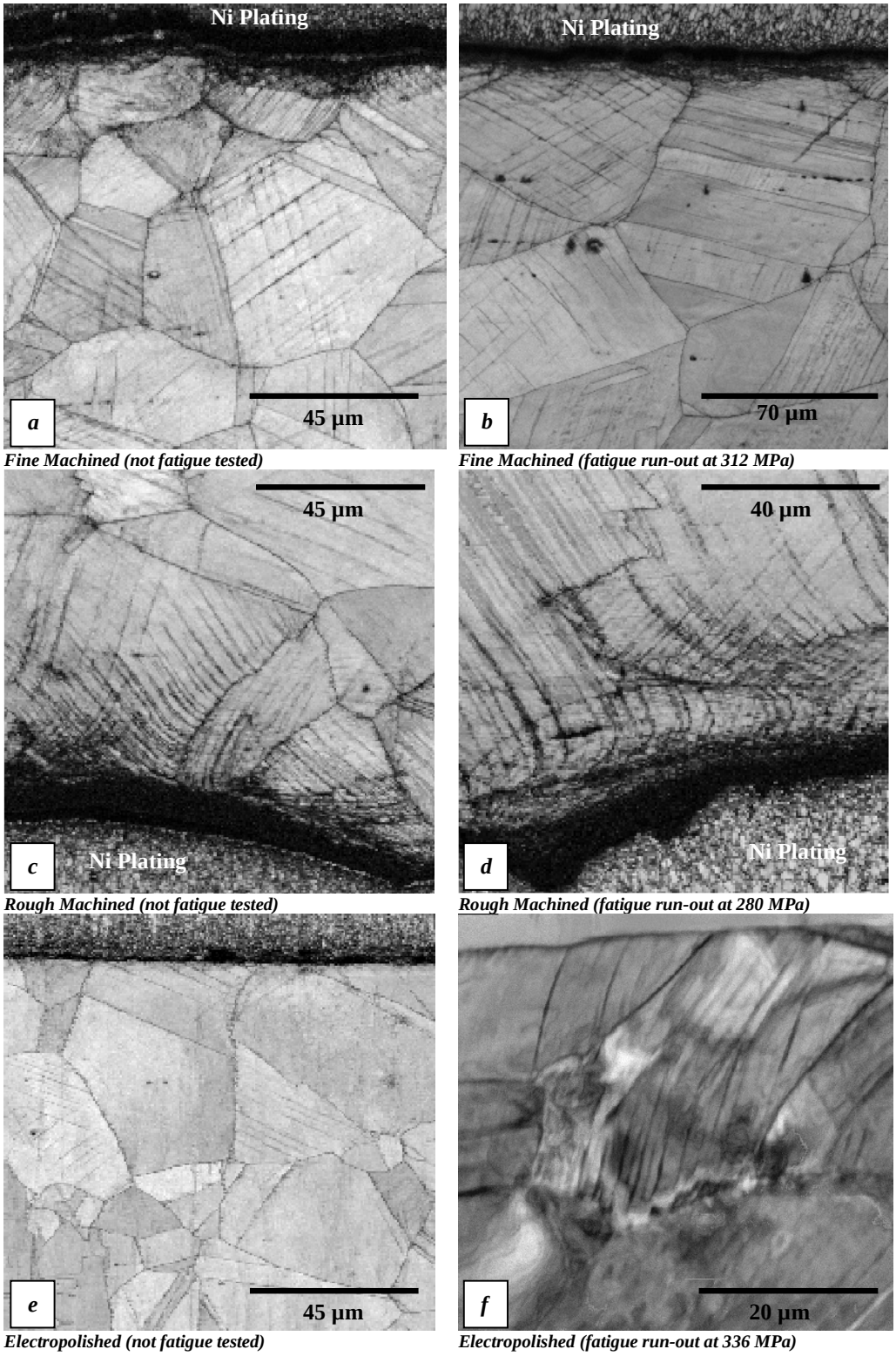

Figure 5: Band contrast maps obtained from EBSD analysis of non-tested specimens and specimens that had been fatigue cycled to run-out, close to the fatigue limit.

Fatigue at the high stresses close to the fatigue endurance limit in austenitic stainless steels causes the development of a plastically strained microstructure (Figure 5). This is apparent from the small, but observable, effect of fatigue on the diffraction peak width in Figure 3b. It has been proposed [8] that slip bands can act as barriers to fatigue cracks. This implies that there are microstructural barriers in the plastically strained microstructure close to the surface, which may more significant to crack propagation than the austenite grain boundaries. The fatigue limit of annealed and electro-polished samples would therefore influenced by the development of the cyclically plastic strained microstructure. It is assumed that this cyclically deformed structure is not affected significantly by the prior plastic strain from machining. The propagation of short cracks such as those in Figure 4 would therefore be expected to be most sensitive to the surface residual stress in machined samples, and insensitive to surface roughness and compressive residual stress peak. Similarly, the surface roughness in annealed samples would be expected to have no significant effect.

The fatigue data obtained from three type 304 austenitic stainless steels with different microstructures (i.e. this work and [2]) are shown in Figure 7, as a function of the surface residual stress. In Figure 7, the same data are shown in terms of the difference from the intrinsic fatigue limit, which is measured with electropolished, annealed samples. The fine grain size microstructure had a grain size of ~8µm and a bulk hardness in the annealed, electropolished condition of 240 Hv; the coarse grain size microstructure had a grain size of ~40µm and a bulk hardness of 200 Hv. These data show that the surface residual stress is a dominant factor in determining the effects of machining on the fatigue limit, for microstructures that had intrinsic fatigue limits between approximately 300 MPa and 385 MPa.

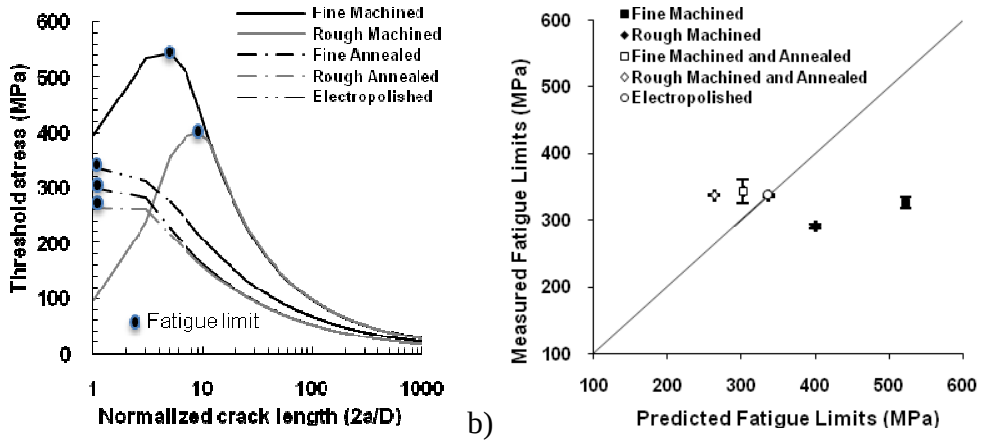

Figure 6: a) Threshold stress profiles predicted for; as machined specimens, annealed specimens and electropolished specimens, b) Predicted fatigue limit in comparison with the measured fatigue limit (N-R Model).

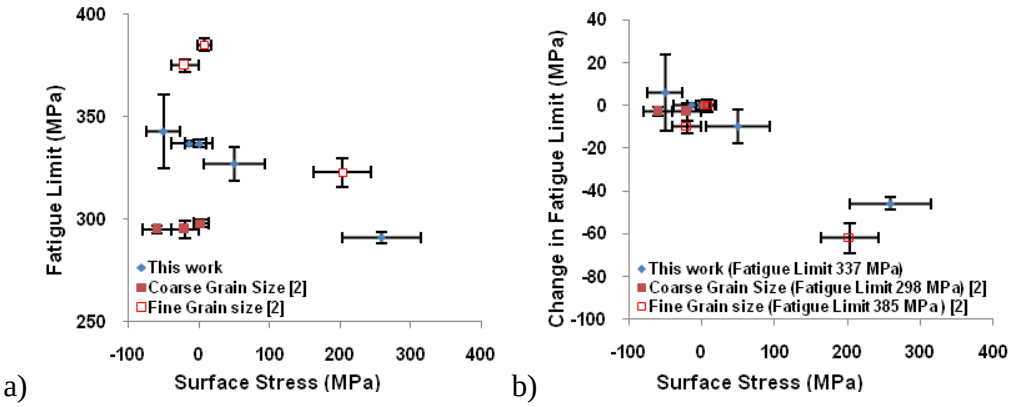

Figure 7: The effect of surface residual stress on the fatigue limit, a) measured fatigue limit b) change in fatigue limit relative to the intrinsic fatigue limit for annealed and electropolished samples.

5. CONCLUSION

Rough machining on a lathe, using a high feed rate, introduced significant tensile residual stress at the machined surface of a type 304L austenitic stainless steel. This significantly decreased the fatigue endurance limit (10^7 cycles). The surface residual stress is found to be the dominant factor controlling this reduction in fatigue resistance, with no measurable effects of surface roughness nor surface cold work. This is explained by a significant interaction between the crack nuclei and the cyclic plastic deformation of the microstructure, which limits the stable crack nucleus size to the near surface region. The effect of surface machining on the fatigue limit of different type 304 austenitic stainless steels can be estimated using the intrinsic fatigue limit for annealed/electropolished samples and the measured surface residual stress. The effects of machining parameters on this surface residual stress can be estimated also using a response surface empirical model.

Acknowledgements

The authors would like to thank Saudi Basic Industries Corporation (SABIC) for financial support of S A-S.

6. REFERENCES

[1] M. Kuroda, T.J. Marrow, Modeling the effects of surface finish on fatigue limit in austenitic stainless steels, Fatigue Fract Engng Mater Struct. 31 (2007), 1-18.

[2] M. Kuroda, T.J. Marrow, Analyses of the effects of surface finish on fatigue limit in austenitic stainless steels by mechanistic modeling, 9th International Fatigue Congress, Atlanta, (2006) USA.

[3] M. Kuroda, T.J. Marrow and A.H. Sherry, Effects of surface finish on fatigue in austenitic stainless steels, 16th European Conference on Fracture, ECF16, Alexandropoulis, Greece, (2006), Ed. E.E. Gdoutos

[4] M. Kuroda, T.J. Marrow, Preparation of Fatigue specimens With Controled Surface Characteristics, Journal of Materials Processing Tech, 203 (2008), 396-403.

[5] M G Moore, W P Evans, Mathematical correction for stress in removed layers in X-ray diffraction residual stress analysis, SAE Trans, 66 (1958) 340-345

[6] R. M'Saoubi , L. Ryde, Application of the EBSD technique for the characterisation of deformation zones in metal cutting, Materials Science and Engineering A. (405) (2005) 339–349.

[7] A. Yamamoto, T. Yamada, Nakahigashi, Li Liu, M. Terasawa and H. Tsubakino, Effects of Surface Grinding on Hardness Distribution and Residual Stress in Low Carbon Austenitic Stainless Steel SUS316L, ISIJ International, (44) (2004), 1780–1782.

[8] J.P. Lucas, and W.W Gerberich, Proposed criterion for fatigue threshold: dislocation substructure Fatigue of Engineering Materials and Structures, 6, (1983), 271-280